ORIGINAL RESEARCH

A novel approach to target hypoxic cancer cells via combining β-oxidation inhibitor etomoxir with radiation

Arpit Dheeraj[1,2]
Chapla Agarwal[1]
Isabel R Schlaepfer[3]
David Raben[4]
Rana Singh[2]
Rajesh Agarwal[1]
Gagan Deep[5–7]

[1]Department of Pharmaceutical Sciences, Skaggs School of Pharmacy and Pharmaceutical Sciences, University of Colorado Anschutz Medical Campus, Aurora, CO, USA; [2]School of Life Sciences, Jawaharlal Nehru University, New Delhi, India; [3]Division of Medical Oncology, University of Colorado Anschutz Medical Campus, Aurora, CO, USA; [4]Department of Radiation Oncology, University of Colorado Anschutz Medical Campus, Aurora, CO, USA; [5]Department of Cancer Biology, Wake Forest School of Medicine, Winston-Salem, NC, USA; [6]Department of Urology, Wake Forest School of Medicine, Winston-Salem, NC, USA; [7]Wake Forest Baptist Comprehensive Cancer Center, Winston-Salem, NC, USA

Correspondence: Gagan Deep
Wake Forest Baptist Comprehensive Medical Center, Hanes 5048, Medical Center Boulevard, Winston-Salem, North Carolina 27157, NC, USA
Tel +1 336 716 9363
Fax +1 336 716 4480
Email gdeep@wakehealth.edu

Background: Hypoxia in tumors is associated with resistance towards various therapies including radiotherapy. In this study, we assessed if hypoxia in cancer spheres could be effectively reduced by adding etomoxir (a β-oxidation inhibitor) immediately after cell irradiation.

Methods: We employed cancer cells' sphere model to target hypoxia. Confocal imaging was used to analyze hypoxia and expression of specific biomarkers in spheres following various treatments (radiation and/or etomoxir).

Results: Etomoxir (32.5 µM) treatment improved the radiation (2.5 Gy) efficacy against growth of lung adenocarcinoma H460 spheres. More importantly, radiation and etomoxir combination significantly reduced the hypoxic regions (pimonidazole+ areas) in H460 spheres compared to either treatment alone. Also, etomoxir and radiation combination treatment reduced the protein level of biomarkers for proliferation (Ki-67 and cyclin D1), stemness (CD44) and β-oxidation (CPT1A) in H460 spheres. We observed similar efficacy of etomoxir against growth of prostate cancer LNCaP cells' spheres when combined with radiation. Further, radiation treatment strongly reduced the hypoxic regions (pimonidazole+ areas) in CPT1 knockdown LNCaP cells' spheres.

Conclusions: Together, these results offer a unique approach to target hypoxia in solid tumors via combining etomoxir with radiation, thereby improving therapeutic efficacy.

Keywords: Hypoxia, radiation, β-oxidation, Etomoxir, CPT1A

Introduction

Hypoxia (low oxygen condition) in solid neoplasms is an early phenomenon, which induces genetic and epigenetic changes in cancer cells and various tumor microenvironment components leading to increased angiogenesis, stemness, metabolic alterations, and selection of resistant clones.[1] Tumor hypoxia status and hypoxia-related biomarkers are associated with poor prognosis, treatment failure, and disease relapse.[1] For example, Hung et al reported that higher hypoxia-inducible factor-1 alpha (HIF-1α) expression in lung cancer patients was associated with a shorter recurrence-free survival.[2] Turaka et al also reported that hypoxia in prostate cancer (PCa), that is, low mean hypoxic prostate/muscle pO_2 ratio, significantly predicts poor long-term biochemical outcome.[3] Milosevic et al reported that tumor hypoxia is associated with early biochemical relapse after radiotherapy and predicts local recurrence.[4] Similarly, several other studies have shown that hypoxia is involved in radioresistance in various cancers.[5–9] Therefore, it is important to simultaneously target hypoxia in tumors along with various therapies for effective treatment and better outcomes.

Several approaches have been tried to overcome or target hypoxia or hypoxia-induced signaling in tumors. Numerous specific or nonspecific inhibitors of HIF-1α and HIF-2α

have been tested to improve the efficacy of various therapies against cancer.[10] For example, YC-1 treatment reduced radiation-induced HIF-1α activation and delayed tumor growth.[11] Similarly, the selective inhibitor of Ataxia telangiectasia and Radd3-related protein (ATR), VE-821, increased the radiation-induced loss of cell viability under hypoxic conditions in different cancer cells.[12] These studies confirm that tumor hypoxia is an important target to overcome radioresistance and to improve the therapeutic efficacy of fractionated radiation. However, one unique challenge is the delivery of these pharmacological agents (HIF-1α or ATR inhibitors) to hypoxic cells as hypoxic areas have reduced blood supply and are mostly beyond the diffusion limit for drug penetrance to hypoxic core. Therefore, additional and novel measures are warranted to better target hypoxic cancer cells.

A complex metabolic reprogramming is an essential feature of cancer cells to satisfy the demand of energy and macromolecules for sustained proliferation under extreme tumor microenvironment.[13,14] Especially, many facets of lipid metabolism including accumulation of lipid droplets, lipogenesis, and β-oxidation, are important in the survival and adaptation of cancer cells to low oxygen conditions.[15–18] We have recently reported that PCa cells accumulate lipids under hypoxia in association with increased HIF-1α, ATP-citrate lyase, and fatty acid synthase expression.[19] We also reported that PCa cells rapidly used their stored lipids for proliferation following reoxygenation of hypoxic cells. Importantly, inhibition of carnitine palmitoyltransferase 1 (CPT1) by etomoxir and stable CPT1 knockdown resulted in compromised growth of hypoxic PCa cells following reoxygenation.[19] These studies suggested that hypoxic cancer cells could be effectively targeted by etomoxir following reoxygenation. To evaluate this hypothesis, in the present study, we combined etomoxir with radiation treatment in a spheroid model, where radiation would reduce the sphere size and reoxygenate the hypoxic cells resulting in elimination by etomoxir treatment due to their dependence on β-oxidation for their survival. Results showed that etomoxir added to radiation could effectively reduce hypoxia and inhibit cancer cell growth in a sphere model.

Methods and materials
Reagents and cell culture
Human lung epithelial carcinoma H460 and prostate carcinoma LNCaP cells were from ATCC (American Type Culture Collection, Manassas, VA, USA) and cultured in Roswell Park Memorial Institute (RPMI) 1640 medium with 10% fetal bovine serum (FBS) and 1% penicillin–streptomycin antibiotics. RPMI1640, FBS, DMEM/F12, penicillin–streptomycin antibiotics, trypsin (0.25% and 0.05%), B27, N2, recombinant epidermal growth factor, fibroblast growth factor, Alexa Fluor 488/594 secondary antibodies, and gold antifade reagent with 4′,6-diamidino-2-phenylindole (DAPI) were from Life technologies (Grand Island, NY, USA). Etomoxir was from Sigma Aldrich Co. (St. Louis, MO, USA). Pimonidazole was from Hypoxyprobe Inc. (Burlington, MA, USA). Primary antibody for cyclin D1 was from Cell Signaling Technologies (Beverly, MA, USA), CD44 from Santa Cruz Biotechnology (Dallas, TX, USA), CPT1A from Proteintech (Rosemont, IL, USA), and Ki-67 from Abcam (Cambridge, MA, USA).

Spheroid culture assay
H460 cells (2,500–5,000 cells/well) or LNCaP cells (10,000 cells per well) were seeded in ultralow attachment six-well culture plates (Corning, St. Louis, MO, USA) in stem cell media (DMEM/F12 media supplemented with B27 and N2). Additionally, for LNCaP spheroid culture, 0.5 mL media with recombinant EGF (20 ng/mL) and FGF (10 ng/mL) were added every 72 h. At day 7 (or as indicated), spheres were irradiated (2.5 Gy as a single fraction dose) using an RS 2000 Biological Irradiator (Rad Source Technologies, Buford, Georgia 30518, USA). Spheres were immediately treated with etomoxir (experiment day 0) and every 48 h thereafter. At the end, sphere numbers was counted and spheres' area was measured using AxioVision Release 4.7 software. A brief summary of the experimental scheme is shown in Figure 1A.

For second-generation spheres, primary spheres were collected by brief centrifugation and incubated with trypsin (0.05%) for 5 min with frequent gentle pipetting to dissociate the spheres. Once the single cells were formed, cells were counted and replated in ultralow attachment plates as described above. Cells were treated with etomoxir 32.5 μM after 24 h of seeding and every 48 h thereafter. The number of spheres was counted after day 6 of treatment.

Clonogenic assay
Spheres were dissociated, counted, and seeded in 6-well plates (1 × 10³ cells/well) in regular culture media. Cells were treated as indicated, and at the end of day 7, cells were fixed with 4% formalin, stained with 1% crystal violet, and colonies with ≥50 cells were counted under a microscope.

Hypoxia staining with pimonidazole
Spheres were treated with pimonidazole (200 μM) for 2 h. Thereafter, spheres were centrifuged at 1,000 rpm for 5 min and fixed in 4% buffered formalin. Next, spheres were transferred in eight-well chamber slides coated with a thin layer of matrigel, permeabilized with PBS with Tween 20 (PBST;
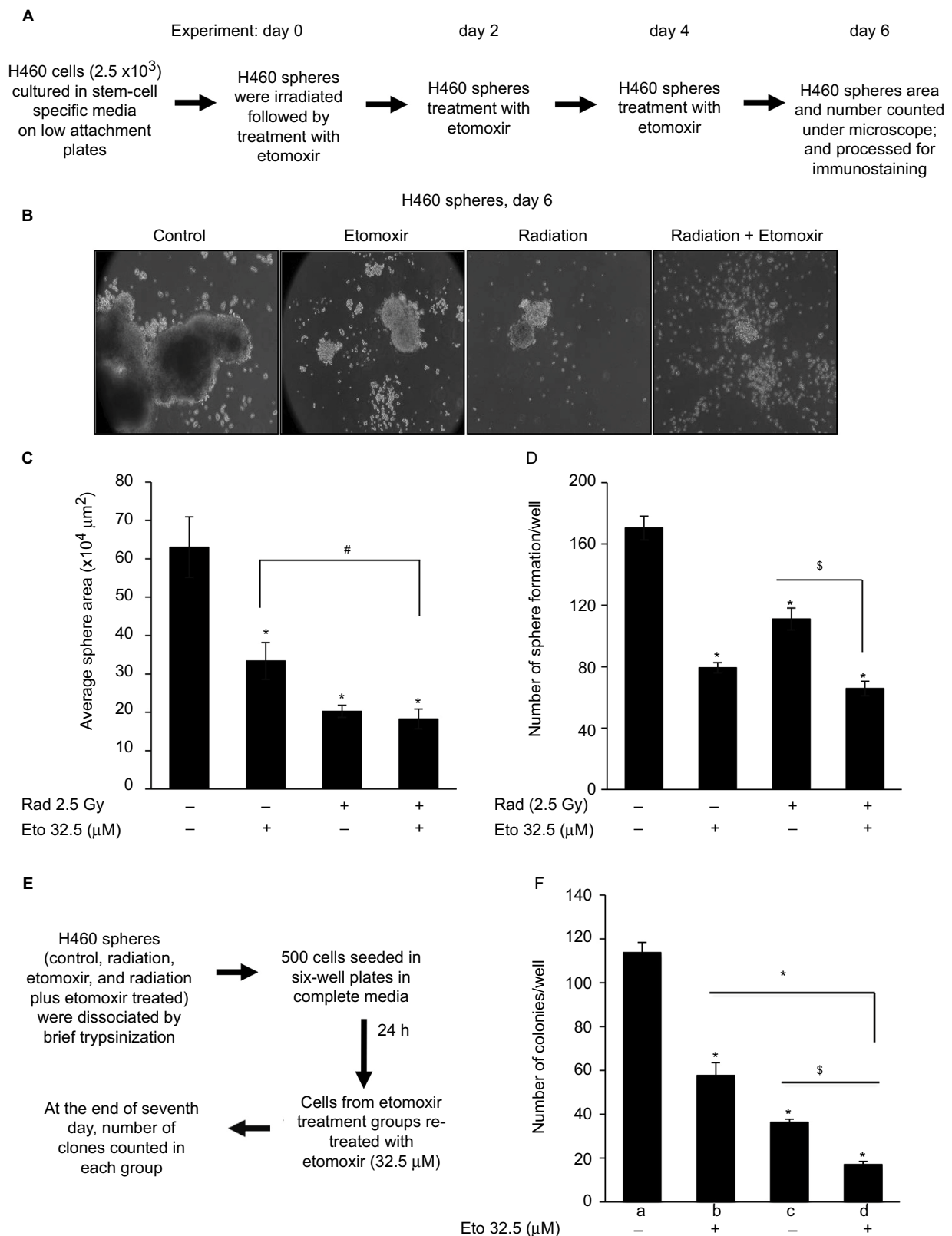
A

Experiment: day 0   day 2   day 4   day 6

H460 cells (2.5 ×10^3) cultured in stem-cell specific media on low attachment plates → H460 spheres were irradiated followed by treatment with etomoxir → H460 spheres treatment with etomoxir → H460 spheres treatment with etomoxir → H460 spheres area and number counted under microscope; and processed for immunostaining

H460 spheres, day 6

B

Control   Etomoxir   Radiation   Radiation + Etomoxir

C

Y-axis: Average sphere area (×10^4 μm^2)

| Rad 2.5 Gy | − | − | + | + |
| Eto 32.5 (μM) | − | + | − | + |

D

Y-axis: Number of sphere formation/well

| Rad (2.5 Gy) | − | − | + | + |
| Eto 32.5 (μM) | − | + | − | + |

E

H460 spheres (control, radiation, etomoxir, and radiation plus etomoxir treated) were dissociated by brief trypsinization → 500 cells seeded in six-well plates in complete media → 24 h → Cells from etomoxir treatment groups re-treated with etomoxir (32.5 μM) → At the end of seventh day, number of clones counted in each group

F

Y-axis: Number of colonies/well

| | a | b | c | d |
| Eto 32.5 (μM) | − | + | − | + |

Figure 1 Etomoxir combination improves radiation efficacy against sphere formation by H460 lung epithelial cancer cells.
Notes: (**A**) Experimental scheme. (**B**) At the end of experiment (day 6), sphere images were captured and representative images are presented (100×). (**C**) Average sphere area presented as mean±SEM. (**D**) Number of spheres in each group presented as mean±SEM. (**E**) Experimental scheme. (**F**) At the end of 7 days, number of colonies with ≥50 cells were counted and presented as mean±SEM in the bar diagram. In the bar diagram, a represents control group, b represents etomoxir alone, c represents radiation alone, and d represents radiation plus etomoxir.*$p<0.001$; $^\$p<0.01$; $^\#p<0.05$.
Abbreviations: Eto, etomoxir; Rad, radiation; SEM, standard error of the mean.

1× PBS + 0.3% Triton X-100) followed by blocking in 5% bovine serum albumin (BSA) block buffer (PBS + 0.3% Triton X-100 + 5% BSA). Spheres were then incubated with fluorescein isothiocyanate-conjugated monoclonal antibody against pimonidazole for overnight and mounted with gold antifade reagent with DAPI. Stained spheres images were captured at 200× magnification using a Nikon D-Eclipse C1 confocal microscope and analyzed using EZ-C1 Free viewer.

Confocal imaging

Spheres were collected, transferred to eight-well chamber slides coated with matrigel, and permeabilized as above. Thereafter, blocking was performed in 5% BSA block buffer (PBS + 0.3% Triton X-100 + 5% BSA). Next, spheres were incubated with respective primary antibodies, Ki-67 (1:100), cyclin D1 (1:200), CD44 (1:100), or CPT1A (1:200) in PBST (with 1% BSA) overnight in a humidified chamber. Thereafter, spheres were incubated with Alexa-Fluor 488 or 594 secondary antibody (1:250) with DAPI (1:1,000) for 1 h and mounted with prolong gold antifade reagent with DAPI. Stained spheres were imaged using a Nikon D-Eclipse C1 confocal microscope and analyzed using EZ-C1 free viewer software. Z stacking was done by complete scanning of spheres in depth, and then a reference point was selected in middle where scans of 5 μm interval were taken in both directions. The fluorescence intensity was quantified using ImageJ software (NIH, Bethesda, MD, USA).

Statistical analysis

Statistical analysis was performed using SigmaStat 2.03 (Jandel Scientific, San Rafael, CA, USA). Data were analyzed by one-way analysis of variance (ANOVA) (Tukey test) and statistically significant differences were considered at $p < 0.05$.

Results

Etomoxir enhances radiation cytotoxicity

Lung adenocarcinoma H460 cells were cultured as spheres to serve as a three-dimensional (3D) model to study hypoxia and effect of radiation and etomoxir treatment. Spheres were irradiated one time with a 2.5 Gy dose (experiment day 0) followed by treatment with vehicle (dimethyl sulfoxide [DMSO], 0.1%) or etomoxir (32.5 μM). Thereafter, spheres were treated with DMSO or etomoxir on experiment days 2 and 4 (Figure 1A). At the end of the sixth day, sphere number and average sphere area were determined. As shown in Figure 1B and C, radiation exposure reduced the average H460 sphere area by 67.87% ($p < 0.001$), and etomoxir combination further reduced the sphere area by 71.04% ($p < 0.001$) compared with control.

Etomoxir alone treatment reduced the sphere area by 47.06% ($p < 0.001$). Further, radiation treatment reduced the H460 sphere number by 34.78% ($p < 0.001$), while combination with etomoxir reduced the sphere number by 61.37% ($p < 0.001$) compared with control; etomoxir alone treatment reduced the sphere number by 53.41% ($p < 0.001$; Figure 1D).

Next, we assessed the colony forming ability of spheres after completion of treatments (vehicle, radiation, etomoxir, or radiation plus etomoxir). In the clonogenic assay, only etomoxir treatment was replenished (wherever mentioned) for continuous inhibition of β-oxidation (experimental scheme shown in Figure 1E). The etomoxir alone-treated single cells of spheres showed reduced capacity to form colonies by 49.27% ($p < 0.001$), while irradiated (2.5 Gy) sphere cells showed reduced clonogenic potential by 68.04% ($p < 0.001$). The combination of radiation and etomoxir further inhibited the clonogenic potential of cells from spheres by 85.05% ($p < 0.001$), and the combined inhibitory effect was significantly better than either radiation or etomoxir alone (Figure 1F). These results further suggested the inhibition of β-oxidation by etomoxir could improve the cytotoxic effect of radiation against cancer cells.

Etomoxir combination with radiation reduces hypoxic areas

Next, we examined the effect of etomoxir treatment along with radiation on hypoxia by staining spheres with pimonidazole. Pimonidazole, a hypoxia marker, is a 2-nitroimidazole compound which forms covalent bond with peptide thiols at oxygen levels below 1.3% and can visualize poorly oxygenated regions in histological samples.[20,21] Spheres were incubated with pimonidazole (200 μM) for 2 h and then processed as described in the "Methods" section. As shown in Figure 2, hypoxic areas were present in spheres treated with radiation alone; however, combination of etomoxir with radiation reduced the hypoxic areas by 59% compared with control spheres. The radiation and etomoxir combination effect was significantly better than either radiation or etomoxir alone (Figure 2).

Etomoxir combination with radiation reduces the expression of proliferation, stemness, and β-oxidation biomarkers

H460 spheres treated with radiation alone showed higher Ki-67 expression compared with control; whereas, spheres treated with etomoxir (32.5 μM) in combination with radiation showed reduced Ki-67 expression compared with radiation treatment alone (Figure 3A and quantification
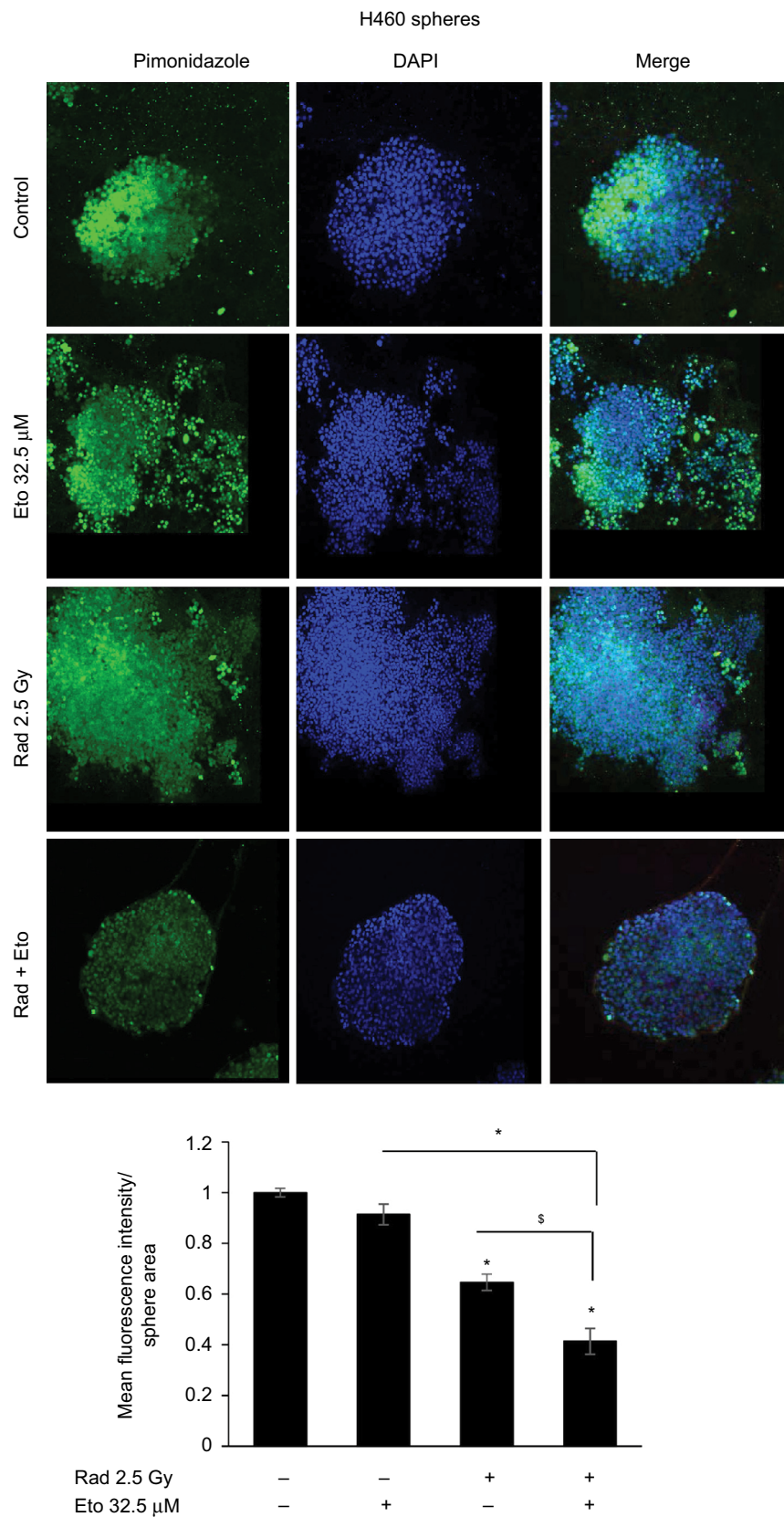
H460 spheres

Figure 2 Etomoxir treatment following radiation exposure reduces hypoxic areas in H460 spheres.
Notes: H460 spheres were irradiated (2.5 Gy) and then treated with etomoxir 32.5 µM. Spheres were re-treated with etomoxir on experiment day 2 and 4. At the end of day 6, H460 spheres were treated with pimonidazole (200 µM) for 2 h and then processed for immunofluorescence. Representative confocal images are shown (at 200× magnification). The bar diagram represents the mean fluorescence intensity per unit sphere area as mean±SEM. *$p<0.001$; $^\$p<0.01$.
Abbreviations: DAPI, 4′,6-diamidino-2-phenylindole; Eto, etomoxir; Rad, radiation; SEM, standard error of the mean.
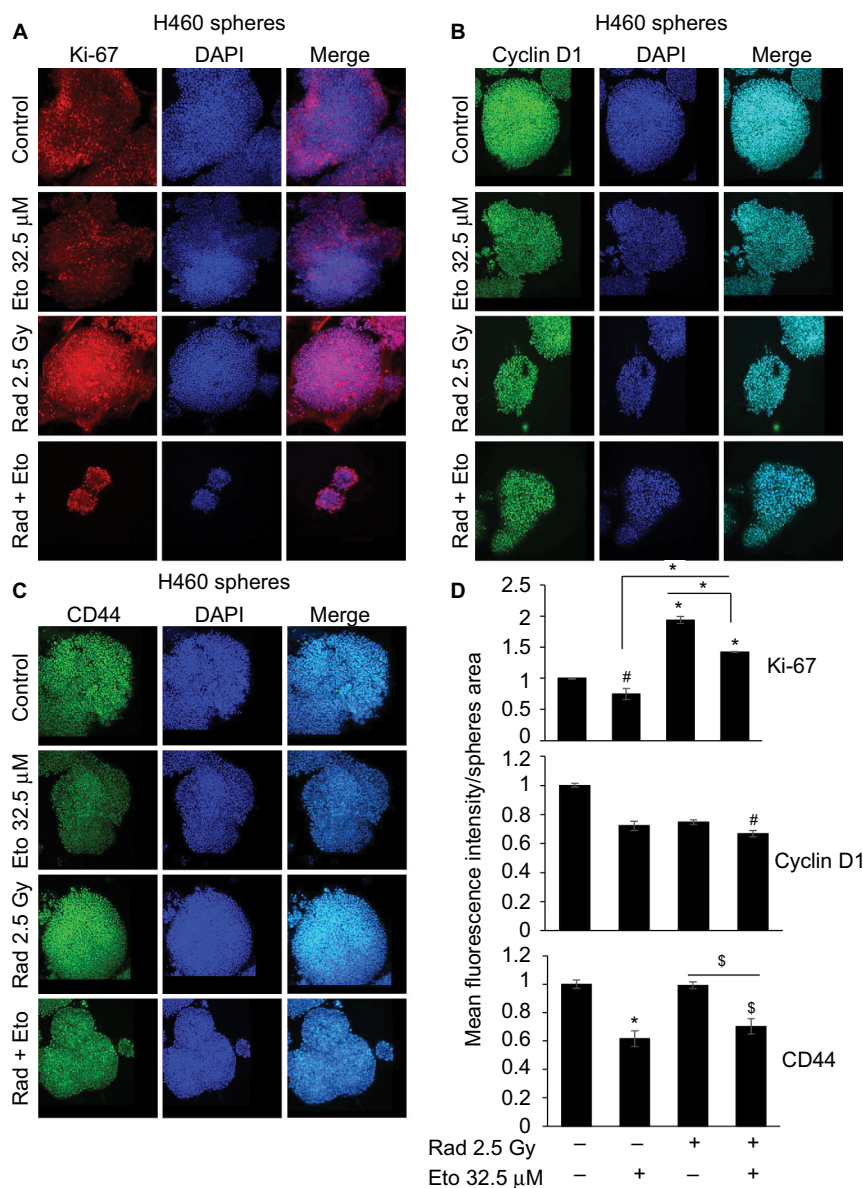
Figure 3 Etomoxir treatment following radiation exposure reduces the expression of proliferation and stemness biomarkers in H460 spheres.

Notes: (**A–C**) 5×10^3 H460 cells were plated in six-well ultralow attachment plates for sphere formation for 6 days. Thereafter, spheres were irradiated with a dose of 2.5 Gy and then treated with etomoxir 32.5 μM. Spheres were retreated with etomoxir on experiment days 2 and 4. At the end of day 6 after first etomoxir treatment, H460 spheres were processed to analyze (**A**) Ki-67, (**B**) cyclin D1, and (**C**) CD44 expression by immunofluorescence as described in the "Methods" section. Representative images are shown (at 200× magnification). (**D**) The bar diagram represents the mean fluorescence intensity per unit sphere area for Ki-67, cyclin D1, and CD44 as mean±SEM. *$p<0.001$; $^\$p<0.01$; $^\#p<0.05$.

Abbreviations: DAPI, 4′,6-diamidino-2-phenylindole; Eto, etomoxir; Rad, radiation; SEM, standard error of the mean.

shown in Figure 3D). Cyclin D1 fluorescence intensity was not significantly affected by etomoxir or radiation alone treatment but the combination showed a significant decrease in cyclin D1 level compared with control (Figure 3B and quantification shown in Figure 3D). Further, etomoxir alone treatment reduced the level of CD44 in H460 spheres; however, radiation alone treatment did not affect the CD44 expression (Figure 3C). The combination of etomoxir and radiation treatment reduced the CD44 expression compared

with radiation treatment alone (Figure 3C and quantification shown in Figure 3D).

As expected, etomoxir treatment alone strongly reduced the CPT1A expression (a biomarker for β-oxidation) in spheres (Figure 4). However, spheres treated with radiation alone showed higher CPT1A expression (Figure 4). Importantly, the combination of etomoxir with radiation effectively reduced the CPT1A expression compared with the radiation alone group (Figure 4).
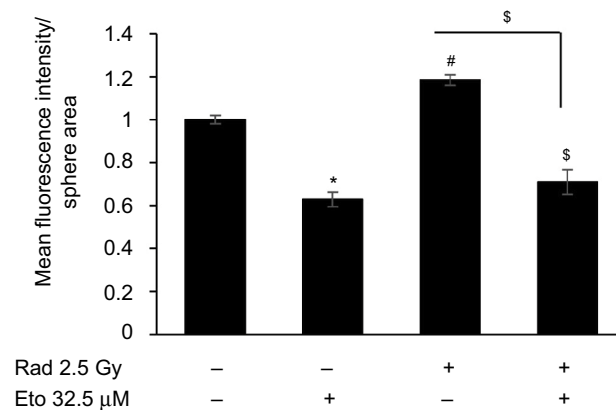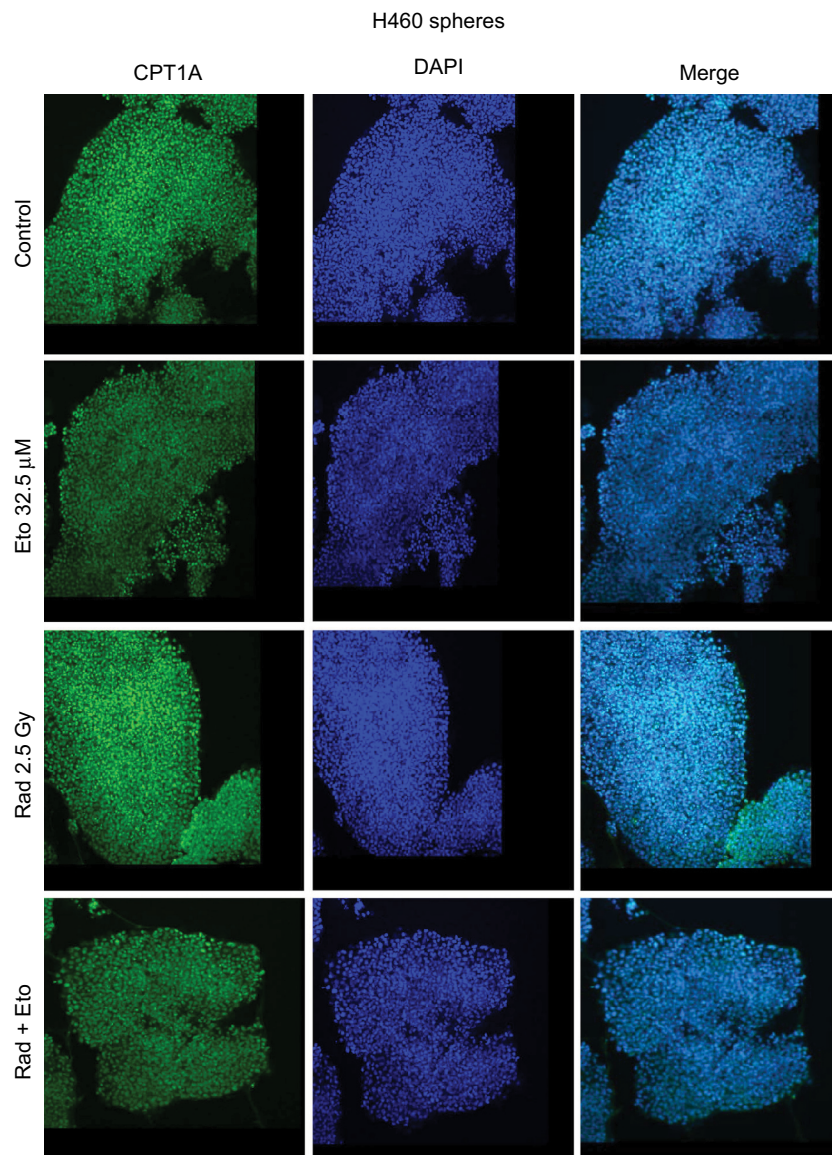
Figure 4 Etomoxir treatment following radiation exposure reduces CPT1 expression in H460 spheres.

Notes: 5×10^3 H460 cells were plated in six-well ultralow attachment plates for sphere formation for 6 days. Thereafter, spheres were irradiated with a dose of 2.5 Gy and then treated with etomoxir 32.5 µM. Spheres were retreated with etomoxir on experiment days 2 and 4. At the end of day 6 after first etomoxir treatment, H460 spheres were processed to analyze CPT1A expression by immunofluorescence as described in the "Methods" section. Representative images are shown (at 200× magnification). The bar diagram represents the mean fluorescence intensity per unit sphere area as mean±SEM. *$p<0.001$; $^{\$}p<0.01$.

Abbreviations: CPT1A, carnitine palmitoyltransferase 1A; DAPI, 4′,6-diamidino-2-phenylindole; Eto, etomoxir; Rad, radiation; SEM, standard error of the mean.

Radiation treatment effectively reduces sphere size and hypoxic areas in CPT1A knockdown LNCaP cells

Subsequently, we confirmed the efficacy of radiation and etomoxir combination to reduce sphere growth in human PCa LNCaP cells. As shown in Figure 5A, radiation alone reduced the sphere number by 39.2% ($p<0.05$), while the combination of radiation and etomoxir reduced the LNCaP sphere number by 47.2% ($p<0.01$). Etomoxir alone treatment reduced the LNCaP sphere number by 28% (Figure 5A). Next, we prepared single-cell suspension of spheres from different treatment groups and seeded in ultralow attachment plates to generate second generation spheres. In the second generation spheres, only etomoxir treatment was continued for effective inhibition of β-oxidation. The etomoxir alone treatment inhibited the second generation sphere numbers by 42.4% ($p<0.001$). The total number of second generation spheres was reduced by 76.8% ($p<0.001$) in the radiation only treatment group, and combination of radiation and etomoxir showed 89.3% decrease in the sphere formation ($p<0.001$; Figure 5B).

To further assess CPT1A role, we performed a similar experiment as above in LNCaP cells with stable CPT1A knockdown (LNCaP CPT1A KD). Radiation treatment reduced the sphere number and size in both LNCaP vector control and LNCaP CPT1A KD cells (Figure 5C and D). Interestingly, pimonidazole staining showed that hypoxic areas were significantly reduced following radiation treatment in LNCaP CPT1A KD cells (Figure 5E).

Discussion

Cancer is an extremely complex disease where in addition to several genetic and epigenetic factors, various tumor microenvironment components also affect cancer development and progression. Hypoxia in tumor microenvironment is one such major factor that appears to correlate with tumor growth, progression, and relapse. A variety of approaches have been used to target tumor hypoxia, which include hyperbaric oxygenation (HBO), accelerated radiotherapy with carbogen and nicotinamide (ARCON) (a combination of carbogen breathing and nicotinamide), anemia correction, and antiangiogenic therapy, thereby increasing plasma and tissue oxygen level.[22,23] However, so far, these therapies have not shown significant efficacy in clinic. For example, the effect of HBO is transient and diminishes in minutes, and the pressure is not tolerated by several patients.[23] Similarly, clinical trials with inhibitors of HIF and hypoxia-induced signaling such as PI3K, Akt, and mTOR inhibitors have not shown promising results owing to poor tissue penetration

to reach hypoxic region as well as pharmacokinetics and pharmacodynamics properties of the tested drugs.[10,24] These clinical outcomes have warranted testing additional novel and innovative measures to target hypoxic cells in tumors.

The reprogramming of lipid metabolism in tumor is now being recognized as an important event for tumor cell growth and progression.[25] Cancer cells fulfill their elevated needs of lipids including fatty acids and phospholipids by de novo lipogenesis.[26,27] Cellular lipids also help in survival and proliferation of cancer cells under hypoxia.[18,28,29] We have recently reported that lipid oxidation is important following reoxygenation in the survival and increased proliferation of hypoxic PCa cells.[19] CPT1 is a major regulator of fatty acid oxidation, which translocates fatty acids conjugated with carnitine to the mitochondria where they can be oxidized to produce acetyl-CoA, which then goes to Krebs cycle and produces NADH and FADH2 for oxidative phosphorylation. Hence, targeting CPT1 can inhibit cancer cell growth by limiting the energy supply of the cell. Currently, several CPT1 inhibitors are in clinical use/trials for treatment of heart disease[30] and could be potentially useful for combination cancer therapy along with radiation. We reported that CPT1 knockdown or inhibition by etomoxir makes hypoxia-reoxygenated cancer cells sensitive toward growth inhibition.[19] Results from the present study further showed that etomoxir combination could improve the anticancer efficacy of radiation and reduce the hypoxic areas in spheres.

In the present study, we employed a sphere model to target physiological hypoxia by single fraction radiation and etomoxir. This model is currently widely used to determine the stemness of cancer cells in in vitro conditions.[31–33] The core region of fully grown spheres is less oxygenated and offers a useful model to understand the hypoxia-mediated biological effects such as radioresistance. We confirmed the extent of hypoxia in spheres using pimonidazole, a nitroimidazole compound considered more sensitive than the microelectrode method of oxygen concentration measurement.[34] As expected, hypoxic regions stained with pimonidazole were located primarily in the irradiated spheres, and etomoxir combination reduced the pimonidazole-stained areas. This combination also reduced the expression of proliferation and stemness biomarkers, as well as decreased the CPT1 expression in the spheres. The increased sensitivity to radiation in combination with etomoxir could be through inhibition of fatty acid oxidation in reoxygenated cells resulting in reduced proliferation and stemness. Alternatively, the reduced pAKT observed in CPT1 KD cells[35] could be responsible for increased sensitivity to the radiation treatment. These results suggest CPT1 as a novel target to overcome radioresistance
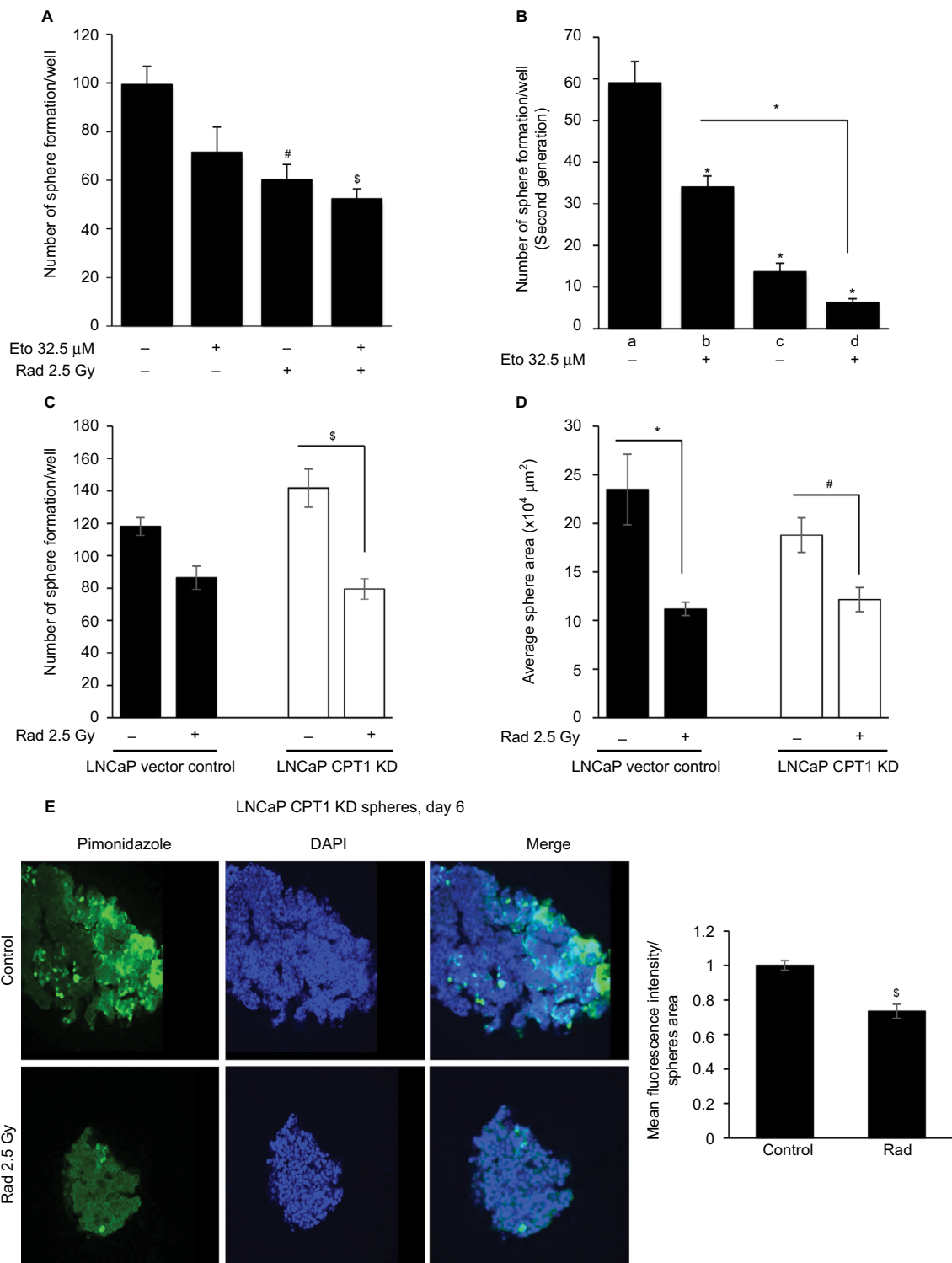
Figure 5 Radiation treatment effectively reduces sphere size and hypoxic areas in CPT1A knockdown LNCaP cells.

Notes: LNCaP spheres were irradiated (2.5 Gy) and then treated with etomoxir 32.5 μM. At the end of day 6, LNCaP spheres number was counted and presented as mean±SEM in the bar diagram (**A**). Thereafter, spheres in each group were dissociated into single cells and plated 1,000 cells/well in ultralow attachment six-well plates. Cells were treated with etomoxir 32.5 μM after 24 h of seeding and every 48 h thereafter. Number of spheres were counted after day 6 of treatment and presented as mean±SEM in the bar diagram (**B**). In the bar diagram, a represents control group, b represents etomoxir alone, c represents radiation alone, and d represents radiation plus etomoxir. (**C, D**) Vector control LNCaP cells and LNCaP CPT1A KD cells were cultured to form spheres and then treated with radiation (2.5 Gy). After 6 days, sphere number and area were measured and presented as mean±SEM in the bar diagrams. (**E**) LNCaP CPT1 KD spheres were treated with 200 μM of pimonidazole for 2 h and processed for immunofluorescence. Representative confocal images are shown (at 200× magnification). The bar diagram represents the mean fluorescence intensity per unit sphere area as mean±SEM. $*p<0.001$; $^{\$}p<0.01$; $^{\#}p<0.05$.

Abbreviations: CPT1A, carnitine palmitoyltransferase IA; DAPI, 4′,6-diamidino-2-phenylindole; Eto, etomoxir; KD, knockdown; Rad, radiation; SEM, standard error of the mean.
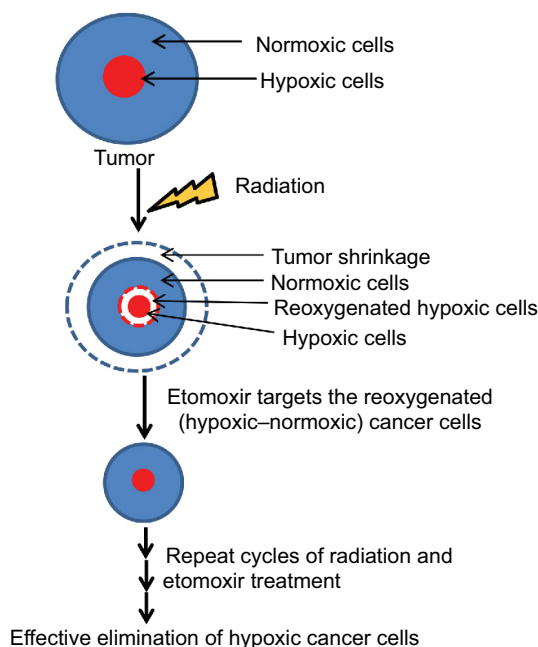
Figure 6 Proposed hypothesis.
Note: Etomoxir, an inhibitor of β-oxidation, treatment following radiation exposure could effectively eliminate hypoxic cells in the tumor, inhibiting tumor growth and preventing disease relapse.

in tumors. The limitation of this model is that spheres are enriched in stem-like cells and might not represent the bulk cancer cells present in solid tumors. However, the success of the radiation and etomoxir against stem cell-enriched spheres, which are relatively difficult to target, further underscores the value of this combination. Furthermore, the applicability of these results to the clinic is much feasible, since clinically approved CPT1 inhibitors like perhexiline or partial β-oxidation inhibitors like ranolazine[36] could be administered to patients concomitantly with their radiation treatment or immediately after.

Conclusion

Results from the present study suggest that combining β-oxidation inhibitor etomoxir with radiation could be a novel and effective strategy for reducing hypoxia in solid tumors (depicted in Figure 6), thereby reducing chances of disease relapse.

Data sharing statement

The datasets analyzed during the current study are available from the corresponding author on reasonable request.

Author contributions

AD performed the experiments and wrote the manuscript; CA contributed in cell culture and manuscript writing; IRS, DR, RS, and RA provided the reagents and contributed in experimental design and manuscript writing; and GD developed the original hypothesis, study design, supervised the experiments, provided reagents, and contributed in manuscript writing. All authors contributed toward data analysis, drafting and revising the paper and agree to be accountable for all aspects of the work.

Disclosure

References

1. Deep G PG. Hypoxia-induced signaling promotes prostate cancer progression: Exosomes role as messenger of hypoxic response in tumor microenvironment. *Crit Rev Oncog.* 2015;20(5–6):419–434.
2. Hung JJ, Yang MH, Hsu HS, Hsu WH, Liu JS, Wu KJ. Prognostic significance of hypoxia-inducible factor-1alpha, TWIST1 and Snail expression in resectable non-small cell lung cancer. *Thorax.* 2009;64(12):1082–1089.
3. Turaka A, Buyyounouski MK, Hanlon AL, Horwitz EM, Greenberg RE, Movsas B. Hypoxic prostate/muscle PO2 ratio predicts for outcome in patients with localized prostate cancer: long-term results. *Int J Radiat Oncol Biol Phys.* 2012;82(3):e433–e439.
4. Milosevic M, Warde P, Menard C, et al. Tumor hypoxia predicts biochemical failure following radiotherapy for clinically localized prostate cancer. *Clin Cancer Res.* 2012;18(7):2108–2114.
5. Brustugun OT. Hypoxia as a cause of treatment failure in non-small cell carcinoma of the lung. *Semin Radiat Oncol.* 2015;25(2):87–92.
6. Lee S-l-o, Ryu H, Son Ar, et al. TGF-β and Hypoxia/Reoxygenation promote radioresistance of A549 lung cancer cells through activation of Nrf2 and EGFR. *Oxid Med Cell Longev.* 2016;2016:6823471.
7. Marampon F, Gravina GL, Zani BM, et al. Hypoxia sustains glioblastoma radioresistance through ERKs/DNA-PKcs/HIF-1alpha functional interplay. *Int J Oncol.* 2014;44(6):2121–2131.
8. Sheehan JP, Shaffrey ME, Gupta B, Larner J, Rich JN, Park DM. Improving the radiosensitivity of radioresistant and hypoxic glioblastoma. *Future Oncol.* 2010;6(10):1591–1601.
9. Li JZ, Gao W, Chan JY-W, Ho W-K, Wong T-S. Hypoxia in head and neck squamous cell carcinoma. *ISRN Otolaryngology.* 2012;2012:8.
10. Wigerup C, Påhlman S, Bexell D. Therapeutic targeting of hypoxia and hypoxia-inducible factors in cancer. *Pharmacol Ther.* 2016;164:152–169.
11. Moeller BJ, Cao Y, Li CY, Dewhirst MW. Radiation activates HIF-1 to regulate vascular radiosensitivity in tumors: role of reoxygenation, free radicals, and stress granules. *Cancer Cell.* 2004;5(5):429–441.
12. Pires IM, Olcina MM, Anbalagan S, et al. Targeting radiation-resistant hypoxic tumour cells through ATR inhibition. *Br J Cancer.* 2012;107(2):291–299.
13. Ward PS, Thompson CB. Metabolic reprogramming: a cancer hallmark even Warburg did not anticipate. *Cancer Cell.* 2012;21(3):297–308.
14. Romero-Garcia S, Lopez-Gonzalez JS, B´ez-Viveros JL, Aguilar-Cazares D, Prado-Garcia H. Tumor cell metabolism. *Cancer Biol Ther.* 2011;12(11):939–948.

15. Bensaad K, Favaro E, Lewis CA, et al. Fatty acid uptake and lipid storage induced by HIF-1alpha contribute to cell growth and survival after hypoxia-reoxygenation. *Cell Rep.* 2014;9(1):349–365.

16. Huang D, Li T, Li X, et al. HIF-1-mediated suppression of acyl-CoA dehydrogenases and fatty acid oxidation is critical for cancer progression. *Cell Rep.* 2014;8(6):1930–1942.

17. Metallo CM, Gameiro PA, Bell EL, et al. Reductive glutamine metabolism by IDH1 mediates lipogenesis under hypoxia. *Nature.* 2012;481(7381): 380–384.

18. Sun RC, Denko NC. Hypoxic regulation of glutamine metabolism through HIF1 and SIAH2 supports lipid synthesis that is necessary for tumor growth. *Cell Metab.* 2014;19(2):285–292.

19. Schlaepfer IR, Nambiar DK, Ramteke A, et al. Hypoxia induces triglycerides accumulation in prostate cancer cells and extracellular vesicles supporting growth and invasiveness following reoxygenation. *Oncotarget.* 2015;6(26):22836–22856.

20. Gross MW, Karbach U, Groebe K, Franko AJ, Mueller-Klieser W. Calibration of misonidazole labeling by simultaneous measurement of oxygen tension and labeling density in multicellular spheroids. *Int J Cancer.* 1995;61(4):567–573.

21. Kizaka-Kondoh S, Konse-Nagasawa H. Significance of nitroimidazole compounds and hypoxia-inducible factor-1 for imaging tumor hypoxia. *Cancer Sci.* 2009;100(8):1366–1373.

22. Moen I, Stuhr LEB. Hyperbaric oxygen therapy and cancer—a review. *Target Oncol.* 2012;7(4):233–242.

23. Baumann R, Depping R, Delaperriere M, Dunst J. Targeting hypoxia to overcome radiation resistance in head & neck cancers: real challenge or clinical fairytale? *Expert Rev Anticancer Ther.* 2016;16(7):751–758.

24. Saggar JK, Yu M, Tan Q, Tannock IF. The tumor microenvironment and strategies to improve drug distribution. *Front Oncol.* 2013;3:154.

25. Beloribi-Djefaflia S, Vasseur S, Guillaumond F. Lipid metabolic reprogramming in cancer cells. *Oncogenesis.* 2016;5:e189.

26. Zaidi N, Lupien L, Kuemmerle NB, Kinlaw WB, Swinnen JV, Smans K. Lipogenesis and lipolysis: the pathways exploited by the cancer cells to acquire fatty acids. *Prog Lipid Res.* 2013;52(4):585–589.

27. Baenke F, Peck B, Miess H, Schulze A. Hooked on fat: the role of lipid synthesis in cancer metabolism and tumour development. *Dis Model Mech.* 2013;6(6):1353–1363.

28. Kamphorst JJ, Chung MK, Fan J, Rabinowitz JD. Quantitative analysis of acetyl-CoA production in hypoxic cancer cells reveals substantial contribution from acetate. *Cancer Metab.* 2014;2:23.

29. Eales KL, Hollinshead KER, Tennant DA. Hypoxia and metabolic adaptation of cancer cells. *Oncogenesis.* 2016;5:e190.

30. Lionetti V, Stanley WC, Recchia FA. Modulating fatty acid oxidation in heart failure. *Cardiovasc Res.* 2011;90(2):202–209.

31. Deep G, Jain AK, Ramteke A, et al. SNAI1 is critical for the aggressiveness of prostate cancer cells with low E-cadherin. *Mol Cancer.* 2014;13(1):37.

32. Bar EE, Lin A, Mahairaki V, Matsui W, Eberhart CG. Hypoxia Increases the Expression of Stem-Cell Markers and Promotes Clonogenicity in Glioblastoma Neurospheres. *Am J Pathol.* 2010;177(3): 1491–1502.

33. Qiang L, Wu T, Zhang HW, et al. HIF-1[alpha] is critical for hypoxia-mediated maintenance of glioblastoma stem cells by activating Notch signaling pathway. *Cell Death Differ.* 2012;19(2):284–294.

34. Raleigh JA, Chou SC, Arteel GE, Horsman MR. Comparisons among pimonidazole binding, oxygen electrode measurements, and radiation response in C3H mouse tumors. *Radiat Res.* 1999;151(5):580–589.

35. Schlaepfer IR, Rider L, Rodrigues LU, et al. Lipid catabolism via CPT1 as a therapeutic target for prostate cancer. *Mol Cancer Ther.* 2014;13(10):2361–2371.

36. Samudio I, Harmancey R, Fiegl M, et al. Pharmacologic inhibition of fatty acid oxidation sensitizes human leukemia cells to apoptosis induction. *J Clin Invest.* 2010;120(1):142–156.